An adaptive flame-tracking shock-capturing scheme for industry-scale explosion simulations

J. Hasslberger, S. Ketterl and T. Sattelmayer
Lehrstuhl für Thermodynamik, Technical University of Munich, 85748 Garching, Germany

1 Introduction

Owing to the large scale disparity between the flame and the confining geometry in large-scale explosion scenarios, it is often impossible to satisfy the best-practice guidelines of turbulent combustion CFD. Thus, special algorithms for flame propagation have to be developed which are less sensitive to insufficient mesh resolution. A well-known example of this category is the CREBCOM model [1] which is available in the COM3D code, for instance. The underlying forest-fire algorithm makes sure that the flame propagates from cell to cell like fire propagates from tree to tree in a forest. A different approach is available in the EUROPLEXUS code [2]. Flame propagation is realized by the reactive discrete equation method which treats the combustion wave as an integral part of a reactive Riemann problem. Another innovative tracking scheme [3] represents a deflagration as a reactive discontinuity embedded in a surrounding compressible flow. Flame propagation is described by the widespread G-equation, i.e. a dynamically evolving scalar function. In this context, the flame is assumed to be the zero level-set of the G field. The costly iterative solution of Rankine-Hugoniot jump conditions is required to couple burned and unburned states within computational cells that are intersected by the front. All mentioned approaches are based on burning velocity correlations to close the combustion source term of the reactive scalar equation.

Following the concept of a *hybrid flame-tracking shock-capturing* scheme in this work, the flame is treated as a reactive discontinuity and explicitly tracked by a geometrical Volume-of-Fluid (VoF) method. In accordance with the URANS framework, the term flame is here used to describe the mean position of the generally turbulent flame brush. Justification of this hybrid approach is based on two observations: First, the equation describing the kinematics of unsteady flame propagation shows a pronounced grid dependency. A strong coupling exists between the flame and other flow properties, especially temperature and density. Hence, it makes sense to devote additional computational resources to accurate flame propagation. Quasi complete removal (to the prescribed tolerance) of numerical dissipation with respect to the reactive scalar equation and therefore a massive reduction of grid sensitivity is demonstrated by the following test cases. Second, the tracking scheme prevents artificial thickening of the turbulent flame brush. The gradient closure of the flamelet source term (eq. 2) does indeed make the reaction rate integral independent of the flame brush width, but it does not avoid unnatural thickening of the flame brush. Whereas this problem does not excessively occur for globally steady combustion (like in stationary burners), it leads to delayed energy release, extenuated thermal expansion and ultimately weaker flame acceleration for globally unsteady combustion (like explosions). If not counteracted by special numerical techniques, the effect amplifies over time and can quickly degrade the solution. In contrast to this problem adherent to flame-capturing, flame-tracking strictly preserves the discontinuous character of the flame independent of mesh resolution.

Correspondence to: josef.hasslberger@gmail.com

2 Methodology

The finite-volume solver is implemented in the open-source CFD package OpenFOAM [4] which is able to handle topologically complex unstructured meshes. Due to the mixed parabolic-hyperbolic nature of explosion problems, the computational methodology is built on the Favre-averaged unsteady compressible Navier-Stokes equations. Conservation of total internal energy and the ideal gas law complete the system of governing equations. Turbulence closure is achieved through the well-established k-ω-SST model [5]. A density-based solver architecture, in combination with a Godunov-type approximate Riemann solver (Harten-Lax-van Leer with Contact scheme [6]; basically treating each cell pair as a shock tube problem) for the calculation of convective fluxes, ensures accurate second-order reproduction of gas-dynamic effects, i.e. shocks. According to their mathematical nature, temporal discretization is explicit with respect to convective terms and implicit with respect to diffusive terms. Dynamic time stepping adjusts the time step size to the accelerating flow. The limiting CFL criterion uses the maximum characteristic wave velocity (convective flow velocity plus speed of sound) in the domain.

In order to reduce overall computational cost, adaptive mesh refinement locally increases the mesh resolution according to the highly unsteady evolution of explosions. A multi-phenomenon refinement criterion is applied to dynamically refine the vicinity of the flame (controlled by gradients of the burned volume fraction) as well as relevant phenomena ahead of the flame, i.e. shock waves (controlled by gradients of unburned density) and regions of enhanced turbulence production (controlled by velocity gradients). Furthermore, the algorithm based on isotropic cell division includes unrefinement in the completely burned region.

Unlike the standard procedure, to solve a conservative transport equation for $\rho\alpha$, the flame is explicitly tracked in this work. Flame propagation is consequently governed by the inhomogeneous advection equation

$$\frac{\partial \alpha}{\partial t} + u_j \frac{\partial \alpha}{\partial x_j} = \max\left(\dot{\omega}_{\mathrm{fl}}; \dot{\omega}_{\mathrm{vol}}\right) \tag{1}$$

for α, the ratio of burned volume to overall volume in each computational cell. Since the solved-for volume fraction α does not directly describe the geometry of the discontinuous front (often termed interface in literature), the latter has to be reconstructed and advected by means of geometric operations. Thus, the applied tracking technique is referred to as a geometrical VoF method. From a historical perspective, the development started with Simple Line Interface Calculation (SLIC) which denotes a piecewise constant approximation of the interface. Spurious behavior of SLIC can especially be observed in vortical flows as the reconstructed local interface is always parallel to one of the mesh lines or coordinate axes. Newer Piecewise Linear Interface Calculation (PLIC) describes a piecewise linear approximation of the interface. Its performance is clearly superior compared to SLIC, since an additional degree of freedom, namely the local orientation of the interface, is included.

To constrain execution of the PLIC scheme to the vicinity of the flame, an identification tolerance ϵ_{id} is introduced, i.e. the costly reconstruction algorithm is only invoked if $\epsilon_{\mathrm{id}} < \alpha < 1 - \epsilon_{\mathrm{id}}$. A planar interface is generally characterized by its orientation and location. The first property is obtained from the gradient of the volume fraction field. To overcome the deficiencies of standard gradient schemes in the context of discontinuous fields, the recently developed Node-Averaged Gauss (NAG) scheme [7] is implemented. In doing so, the shape of arbitrary cell faces is taken into account via a triangulation procedure. Being one of the main advantages, execution of the NAG scheme does not involve costly loops over neighbor cells. Moreover, it works well on arbitrary unstructured meshes and does not require preceding smoothing of the volume fraction field. The second property results from the enforcement of local volume conservation. In each

front cell, the interface is iteratively positioned such that the truncated volume matches the discrete volume fraction value by an iterative tolerance ϵ_{it}. Based on the mathematical description of the planar interfaces by their Hesse normal form, the corresponding offset is determined in an iterative manner. Brent's iteration method [8] has been chosen for this purpose since it guarantees to find a root while showing a quadratic convergence rate for sufficiently smooth problems. The basic idea behind Brent's algorithm is to keep track of the convergence behavior of a super-linear method and to intersperse bisection steps if necessary. In the next step, the volume fluxes between neighbor cells are determined by constructing the so-called flux polyhedrons and intersecting them with the reconstructed local front. Global volume conservation is first improved by conservatively redistributing the small undershoots/overshoots (i.e. if $\alpha < 0$ or $\alpha > 1$) to the surrounding cells. Boundedness of the volume fraction field is finally assured by clipping the remaining undershoots/overshoots. In summary, the implemented approach can be characterized as a directional-unsplit multi-dimensional geometrical VoF method based on conservative PLIC with unstructured mesh support, to be fully consistent with the mesh handling paradigm of OpenFOAM. Especially the mesh flexibility comes at the prize of high algorithmic complexity. A detailed mathematical description of the VoF algorithm can be found in [10].

After completing the advection step, the reaction step is executed. The combustion model is based on a coupling of two source terms accounting for different regimes of turbulence-chemistry interaction. During the initial stage of flame propagation, from low to moderate turbulence intensities, the flamelet assumption is well justified. Compared to the time scales of turbulence, chemical kinetics is clearly faster and thus not the limiting factor. In the course of the explosion process, the interaction of the flame with turbulent eddies intensifies, causing a vertical shift in the Borghi diagram towards higher turbulence intensities and turbulent Karlovitz numbers above unity. Though not reflected by the Borghi diagram, also flame instabilities and auto-ignition effects play an important role during the later stage of flame acceleration. Beyond the flamelet regime, the concept of a flame surface is not valid anymore. The character of the reaction zone becomes more distributed with local conditions similar to a (perfectly) stirred reactor. Under such well-mixed conditions, the reaction rate is limited by chemical kinetics and it is more appropriate to speak of volumetric reaction. The first source term

$$\dot{\omega}_{\text{fl}} = \underbrace{\frac{\rho_u}{\rho} G \Xi S_L}_{S_{\text{eff}}} \left| \frac{\partial \alpha}{\partial x_j} \right|, \tag{2}$$

representing flamelet-like combustion, incorporates different submodels for flame quenching G, flame wrinkling Ξ and quasi-laminar burning velocity S_L (also accounting for the effect of intrinsic flame instabilities via an effective Lewis number approach). It can be shown mathematically that S_{eff} is equivalent to an additional propagation velocity normal to the flame's surface. The second source term

$$\dot{\omega}_{\text{vol}} = \frac{2B}{t_{\text{exo}}} \alpha (1 - \alpha)\ \text{H}(\tau - 1), \tag{3}$$

representing volumetric reaction, is activated by the Heaviside function H when the ignition precursor reaches $\tau = 1$ (two-step formulation). If the characteristic reaction time t_{exo} is defined as the time span in which α rises from 0.01 to 0.99, then $B \approx 4.595$ can be determined from first principles. To avoid the costly runtime-evaluation of numerically stiff source terms (of the Arrhenius type), required quantities of chemical kinetics (e.g. ignition delay times) are provided to the solver as correlations or look-up tables. Since the reaction rate modeling is not at the focus of this paper, the interested reader is referred to [9, 10] for further details. However, it is worth mentioning that the framework of the hybrid flame-tracking shock-capturing scheme is independent of the specific choice of the reaction rate model.

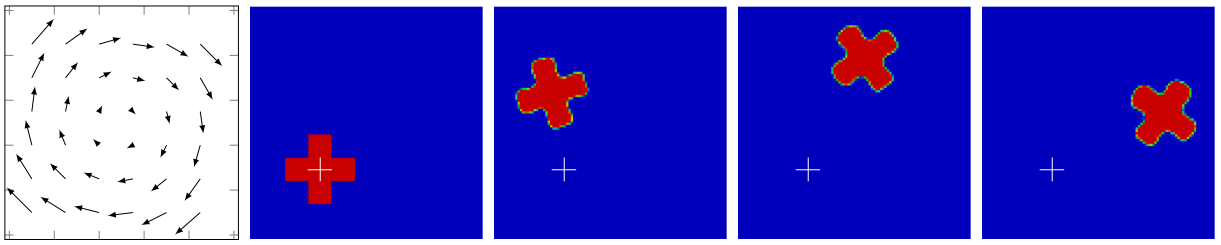

(a) Velocity field (b) $t = 0.0$ s; geom. VoF (c) $t = 0.2$ s; geom. VoF (d) $t = 0.4$ s; geom. VoF (e) $t = 0.6$ s; geom. VoF

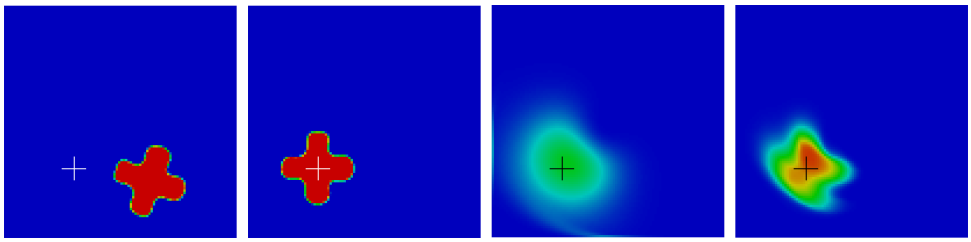

(f) $t = 0.8$ s; geom. VoF (g) $t = 1.0$ s; geom. VoF (h) $t = 1.0$ s; upwind (i) $t = 1.0$ s; TVD

Figure 1: Non-reacting rotating cross example: Velocity field including magnitude-scaled arrows; Volume fraction α at different points in time and by using different discretization schemes; Blue-to-red rainbow color scale from 0 to 1.

3 Fundamental test cases

In one dimension, almost perfect advection of a rectangular profile can be achieved by the VoF technique. The following multi-dimensional cases are more challenging than one-dimensional problems, and designed to reveal benefits and drawbacks of the geometrical VoF method. Dissipation-free propagation with algebraic flux calculation is practically impossible, even with the newest-generation high-order schemes. The first example (fig. 1) relates to the two-dimensional evolution of a sharp initial profile in a constant velocity field given by the stream function

$$\Phi = \frac{\omega}{2}\left((y-y_0)^2 + (x-x_0)^2\right). \tag{4}$$

The velocity components, describing divergence-free rigid body rotation in clockwise direction, can be derived as

$$u_j(x_j) = \begin{pmatrix} \frac{\partial \Phi}{\partial y} \\ -\frac{\partial \Phi}{\partial x} \end{pmatrix} = \begin{pmatrix} \omega \cdot (y-y_0) \\ -\omega \cdot (x-x_0) \end{pmatrix} \tag{5}$$

with $(x_0 = 0, y_0 = 0)$ being the rotation axis and $\omega = 2\pi$/s representing the angular velocity. The analytical solution at $t = 1.0$ s, i.e. after one revolution, is equal to the initial condition. Concerning the volume fraction initial condition, the length of the red cross in one dimension is 0.3 m. The rectangular domain Ω = [−0.5 m, 0.5 m] × [−0.5 m, 0.5 m] is uniformly discretized by 100 × 100 square cells. Hence, interface propagation is generally not aligned with mesh lines, making the problem more challenging than one-dimensional propagation. Pictures (b) to (g) of fig. 1 depict the VoF solution at six points in time. The interface remains sharp, i.e. thickness of the transition region does not grow larger than one cell. The congruent cross position at the beginning and after one revolution means that no noticeable dispersive error occurs. Being a known drawback of all VoF schemes based on piecewise linear interface calculation, sharp

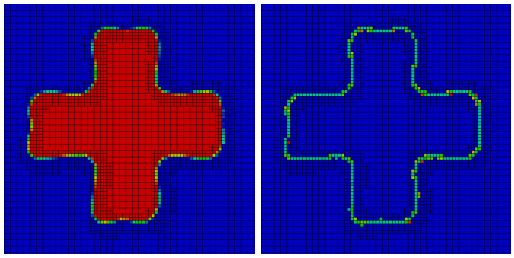

(a) Volume fraction α (b) Iteration counter

Figure 2: Non-reacting rotating cross example: Front tracking combined with level 1 adaptive mesh refinement; Magnified solution and mesh lines at $t = 1.0$ s; Blue-to-red rainbow color scale from 0 to 1 (left picture) and from 0 to 13 (right picture), respectively.

corners are slightly rounded off. In the second row of fig. 1, the geometrical VoF method is opposed to algebraic flux calculation. Representing popular standard schemes, a first-order upwind and a second-order Total Variation Diminishing (TVD) scheme are used for comparison. Significantly higher numerical dissipation can be observed in both cases. Non-bulk cells are spread over a wide range. Especially the upwind scheme is known for its robustness but strong dissipative behavior. The limited TVD scheme suffers to a lesser extent from numerical dissipation but is still clearly inferior to the geometrical VoF scheme. Other TVD schemes (e.g. applying van Leer's limiter) produce similar results. Identification of the cross geometry is hardly possible for the TVD scheme and completely impossible for the upwind scheme. For both schemes, no correct bulk values are preserved. The last picture in fig. 1 reveals the dissipative error which scales with the local velocity magnitude. The solution deteriorates with increasing distance from the rotation axis. Algebraic flux calculation is eventually not an adequate approach to advect discontinuous solutions.

Further improvement can be achieved by combining front tracking with adaptive mesh refinement. In this case, mesh refinement in the vicinity of the interface is controlled by the volume fraction gradient field. Within the general limitations, fig. 2 proves excellent preservation of the cross shape after one revolution. Obviously, the combination of both techniques works as intended.

The computational effort of the VoF technique primarily scales with the number of iterations required to meet the iterative tolerance ϵ_{it} within the reconstruction step. Underlying geometrical operations have to be repeated for each iteration. On the right-hand side, fig. 2 shows the iteration counter in the so-called front cells satisfying the identification tolerance ϵ_{id}. Besides ϵ_{it}, the number of iterations also depends on the volume fraction in the considered cell. The highest number of iterations is required if α is close to zero or unity in front cells. In the presented simulation, the maximum of 13 is considerably higher than the average iteration count of 5.4.

To validate the proper integration of the combustion source term in the volume fraction evolution equation, another test is performed. Both advection and simultaneous reaction (as specified by eq. 2) are taken into account. The setup (mesh, solver settings, velocity field etc.) is the same as before with the exception of the volume fraction initial condition. Here, the cross is replaced by a circle of diameter $d_0 = 0.1$ m. Its center is initially placed at ($x = -0.15$ m, $y = -0.15$ m). According to the constant burning velocity of S_{eff} = 0.1 m/s, the diameter of the circle should grow by $\Delta d = 2\ \Delta r = 2\ S_{\text{eff}}\ \Delta t$ = 2 · 0.1 m/s · 1.0 s = 0.2 m until the simulation ends at $t = 1.0$ s. Figure 3 shows the expected behavior with an end diameter of $d_0 + \Delta d = 0.3$ m. Second, the circle's center correctly arrives at the initial position after one revolution

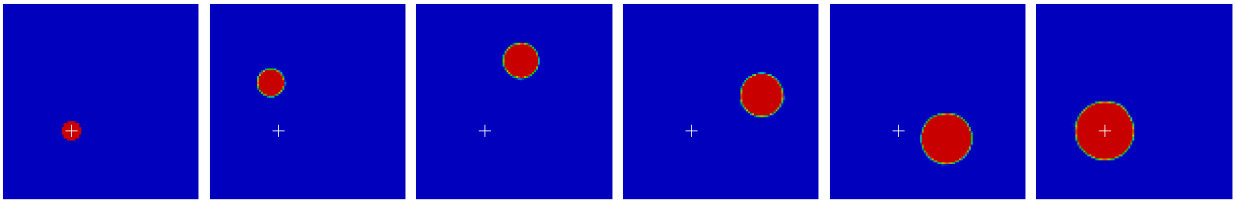

(a) $t = 0.0$ s (b) $t = 0.2$ s (c) $t = 0.4$ s (d) $t = 0.6$ s (e) $t = 0.8$ s (f) $t = 1.0$ s

Figure 3: Reacting rotating circle example: Volume fraction α at different points in time; Blue-to-red rainbow color scale from 0 to 1.

in clockwise direction. Spurious preferred propagation orthogonal to mesh lines does not appear. Both processes, advection and reaction, are well represented by the scheme.

Extensive references and validation of the overall method by means of large-scale explosion experiments in the RUT facility (including the hazardous deflagration-to-detonation transition) can be found in [10]. It appears that DDT by shock focusing can be simulated with reasonable accuracy whereas DDT in the vicinity of the turbulent flame brush is more challenging. Furthermore, the influence of grid resolution as well as the evolution of flame surface area (on both modeled and resolved level) are discussed therein.

References

[1] Efimenko, AA, Dorofeev, SB. (2001). CREBCOM code system for description of gaseous combustion. J. of Loss Prevention in the Process Industries, 14:575–581.

[2] Velikorodny, A, Studer, E, Kudriakov, S, Beccantini, A. (2015). Combustion modeling in large scale volumes using EUROPLEXUS code. J. of Loss Prevention in the Process Industries, 35:104–116.

[3] Smiljanovski, V, Moser, V, Klein, R. (1997). A capturing-tracking hybrid scheme for deflagration discontinuities. Combustion Theory and Modelling, 1:183–215.

[4] Weller, HG, Tabor, G, Jasak, H, Fureby, C. (1998). A tensorial approach to computational continuum mechanics using object-oriented techniques. Computers in physics, 12(6):20–631.

[5] Menter, FR. (1994). Two-equation eddy-viscosity turbulence models for engineering applications. AIAA Journal, 32(8):1598–1605.

[6] Toro, EF, Spruce, M, Speares, W. (1994). Restoration of the contact surface in the HLL-Riemann solver. Shock waves, 4(1):25–34.

[7] Maric, T, Marschall, H, Bothe, D. (2013). voFoam-A geometrical Volume of Fluid algorithm on arbitrary unstructured meshes with local dynamic adaptive mesh refinement using OpenFOAM. arXiv preprint:1305.3417.

[8] Brent, RP. (1971). An algorithm with guaranteed convergence for finding a zero of a function. The Computer Journal, 14(4):422–425.

[9] Ettner, FA. (2013). Effiziente numerische Simulation des Deflagrations-Detonations-Übergangs. PhD thesis. Technical University of Munich.

[10] Hasslberger, J. (2017). Numerical simulation of deflagration-to-detonation transition on industry scale. PhD thesis. Technical University of Munich.
https://www.td.mw.tum.de/fileadmin/w00bso/www/Forschung/Dissertationen/hasslberger2017.pdf